Simultaneous analysis of Si, Mn and Ti segregation in pig iron by laser-induced breakdown spectroscopy

Mei Yaguang[1], Cheng Yuxin[1], Cheng Shusen[1*], Hao Zhongqi[2], Guo Lianbo[2], Li Xiangyou[2], Zeng Xiaoyan[2]

(1. School of Metallurgical and Ecological Engineering, University of Science and Technology Beijing, Beijing 100083, China;
2. Wuhan National Laboratory for Optoelectronics, Laser and Terahertz Technology Division, Huazhong University of Science and Technology, Wuhan 430074, China)

Abstract: There has been no effective method for detecting the element segregation of large metallic material samples so far. In this research, the newly emerging laser-induced breakdown spectroscopy (LIBS) was applied to quantitatively analyze the segregation of Si, Mn and Ti in pig iron simultaneously. The spectra lines of Si (288.16 nm), Mn (293.31 nm) and Ti (334.94 nm) were selected as the quantitative analysis spectral lines, while lines of Fe (263.58 nm, 441.51 nm, 370.79 nm) were chosen as the internal calibration lines to reduce the influence of matrix effect. The fitting correlation coefficients (R^2) were 0.991 7, 0.990 3, 0.991 2, respectively, which proved the ability of LIBS in measuring the concentration of Si, Mn and Ti correctly and simultaneously. A pig iron sample from blast furnace was cut into two round iron samples, whose surface were analyzed with the help of spatial-resolved LIBS subsequently. The element maps revealed the segregation locations of Si, Mn and Ti. The maximum positive and negative segregation degree of three alloy elements was also calculated based on the analysis results of LIBS. The work in this study demonstrates the capability of LIBS for detecting the segregation of alloy elements in pig iron simultaneously. It also reveals the segregation law of alloy elements in pig iron, which is meaningful for the understanding of alloy elements transfer and distribution during solidification process.

Key words: laser-induced breakdown spectroscopy; surface analysis; pig iron; segregation
CLC number: O433.5 Document code: A DOI: 10.3788/IRLA201847.0806003

基于激光诱导击穿光谱技术的生铁中硅锰钛偏析的同步分析

梅亚光[1],程宇心[1],程树森[1*],郝中骐[2],郭连波[2],李祥友[2],曾晓雁[2]

(1. 北京科技大学 冶金与生态工程学院,北京 100083;
2. 华中科技大学 武汉光电国家实验室 激光与太赫兹技术功能实验室,湖北 武汉 430074)

摘 要: 到目前为止,尚没有适用于大型金属材料试样元素偏析定量检测的有效方法。该研究将新兴的激光诱导击穿光谱 (LIBS) 技术应用于生铁中 Si、Mn、Ti 元素偏析的同步检测,选取 Si (288.16 nm)、Mn

收稿日期: 2018-03-10; **修订日期:** 2018-04-20
基金项目: 国家自然科学基金(61571040)
作者简介: 梅亚光(1993-),男,博士生,主要从事激光诱导击穿光谱分析及钢铁冶金工艺方面的研究。Email: myg_ustb@163.com
导师简介: 程树森(1964-),男,教授,博士生导师,博士,主要从事高炉炼铁工艺及冶金自动化设备开发方面的研究。
Email: chengsusen@metall.ustb.edu.cn

(293.31 nm) 和 Ti (334.94 nm)作为三种元素的定量分析谱线,同时选取 Fe (263.58 nm, 441.51 nm, 370.79 nm) 分别作为三种元素的内标谱线, 使用内标法降低基体效应的影响。定标拟合系数 R^2 分别为 0.991 7、0.990 3 和 0.991 2,因此证明 LIBS 适用于对生铁中 Si、Mn、Ti 元素的准确同步定量检测。随后将取自高炉的铁样切割为两个圆形的铁块,用空间分辨的 LIBS 装置对样品表面进行面扫描分析并得出元素分布图,基于元素分布图识别出 Si、Mn、Ti 元素的偏析区域并计算最大正偏析度和负偏析度。该研究证明了 LIBS 用于同步检测生铁中 Si、Mn、Ti 元素偏析的可行性,同时也揭示了生铁中合金元素的偏析规律,有利于加深对凝固过程元素迁移和分布的理解和认识。

关键词:激光诱导击穿光谱; 面扫描; 生铁; 偏析

0 Introduction

The segregation phenomenon is the heterogeneous distribution of elements during alloy solidification process. It is mainly caused by the solute redistribution and inadequate diffusion of elements. In many material processing industries, element segregation is always an important research hotspot. That is due to the serious effect of element segregation on material properties such as toughness, plasticity, welding performance and corrosion resistance. Till now, large amounts of researchers have been studying on the control mechanism of element segregation in all kinds of materials [1-3]. However, it was found that there was't segregation detecting method suitable for engineering application. Take steel industry for example, the methods currently used are sulfur print and carbon drilling, which can't provide quantitative and enough information about element distribution simultaneously.

Laser-induced breakdown spectroscopy (LIBS) is a new analytical technique based on atomic emission spectroscopy. Its prominent ability is rapid, in-situ and simultaneous multi-element detection of element concentration in materials with little sample pretreatment [4]. In the past several decades, this new technology had achieved great development and was applied to the researches in many fields, such as element detection in plants[5], soil[6-7], cement[8], alloy[9-10], mineral[11], water[12], pulverized coal[13-14] and rubber[15] etc. If combined with three-dimensional mobile device, it can also be used for detecting element distribution, based on which the element segregation degree and the segregation regions can be gotten for metallic materials. Some domestic and overseas scholars had conducted researches on application of LIBS on the analysis of element segregation. Fabienne Boué-Bigne[16] analyzed the carbon segregation and decarburization of cast products from continuous casting of high carbon steel with the help of spatially-resolved LIBS. The LIBS system could generate fast scan with a laser pulsing at 1 kHz. Fabienne Boué-Bigne[17] also demonstrated the feasibility of simultaneous analysis of carbon segregation and cementite networks in rolled finished rod products of high carbon steel by LIBS with the help of same LIBS setup. Zhang Yong [18] analyzed the segregation of C, Si, Mn, P, S, Cu and Ti in two middle-low alloy slabs by LIBS. The result proved the ability of LIBS in detecting the segregation band location and its width.

The studies mentioned above proved that LIBS is an ideal technique for analyzing the element segregation in steel. However, pig iron is a kind of material which usually be used for steel-making or casting. Pig iron has much difference with steel in properties and element concentrations even though its matrix is Fe too. The Si, Mn and Ti are three important alloy

elements in blast furnace pig iron. In this work, the segregation of three elements mentioned above in blast furnace pig iron was detected simultaneously with the help of spatially-resolved single pulse LIBS, based on which the segregation law of three alloy elements in pig iron was revealed.

1 Experiment

1.1 LIBS setup

Fig.1 shows a schematic representation of the experimental setup. A Q-switched Nd:YAG laser (Litron laser Nano S) operating at 1 064 nm and 60 mJ per pulse was used to excite the plasma. The repetition rate is 10 Hz. The pulse duration (full width at half-maximum-FWHM) is 8 ns. The output laser was focused by a 150 mm focal lens above the sample with a focal point at 4 mm below the sample surface. The plasma emission was collected by light collector (Ocean Optics, 84-UV-25) and coupled into an echelle spectrometer (LTB ARYELLE200). A 1 024 pixel×1 024 pixel charge-coupled device (Andor Tech., ikon-M 934-BU2) was installed on the spectrometer to acquire the spectra. The time delay between laser and CCD was 2 μs. The pig iron sample was placed on a three-dimensional moving plate for surface scanning by LIBS. Step size as small as 0.1 mm was available in three directions. In this work, 2D surface analysis was carried out with 2 mm between two adjacent ablation points. To reduce the influence of laser energy fluctuation, the spectra was got from the cumulative results of 50 pulses.

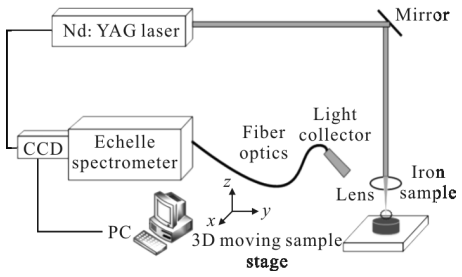

Fig.1 Schematic diagram of the experimental single-pulse LIBS system

1.2 Calibration process

Four groups of standard iron samples (Pangang Group Research Institute Co., Ltd, GSB03-2582-2010 and NCS Testing Technology Co., Ltd, GBW01131a-37a, YSBS20403-06, GBW01594-01600) were used in this study for the calibration of Si, Mn and Ti concentrations in pig iron. The chemical and physical properties of four groups of pig iron samples were similar with each other. In addition, there was small difference between their composition and the manufacturing methods are similar. For convenience, the standard samples groups list above were named from 1 to 4, respectively. Their detailed Si, Mn and Ti concentrations were list in Tab.1.

Tab.1 Reference concentrations of Si, Mn and Ti elements in the standard pig iron samples (wt%)

	1-1	1-2	1-3	1-4	1-5	1-6	1-7
Si	0.099	0.937	0.689	0.451	0.183	0.99	1.85
Mn	0.072	0.329	1.22	0.857	0.596	1.46	2.06
Ti	0.005 9	0.216	0.043	0.03	0.066	0.105	0.399
	2-1	2-2	2-3	2-4	2-5	2-6	2-7
Si	0.93	2.28	1.5	0.246	2.65	3.68	3.35
Mn	0.317	0.715	1.12	0.987	1.27	1.7	1.99
Ti	0.223	0.478	0.388	0.031	0.078	0.129	0.131
	3-1	3-2	3-3	3-4	3-5	3-6	
Si	3.52	2.74	0.907	1.76	0.378	1.21	
Mn	0.248	0.403	0.538	0.9	1.2	0.251	
Ti	-	-	-	-	-	-	
	4-1	4-2	4-3	4-4	4-5	4-6	
Si	3.52	2.59	2.04	1.47	1.01	0.57	
Mn	1.52	1.04	0.52	0.762	0.331	0.103	
Ti	0.082	0.042	0.14	0.16	0.033	0.057	

In this work, the internal standardization was

adopted as the quantitative analysis method. Characteristic spectra lines of Si, Mn and Ti were selected from amounts of lines according to the detailed parameters of spectra lines and previous experience of other researchers. Based on the obtained set of pairs of variates ($I_{Si,\ Mn,Ti}/I_{Fe}$, $C_{Si,\ Mn,Ti}$), calibration curves were determined by regression analysis. Ten detections were conducted in different positions of each standard iron sample and their average intensity ratio ($I_{Si,\ Mn,Ti}/I_{Fe}$) were adopted as the final data for calibration. It aimed to reduce the experimental error such as small element segregation in standard samples or the fluctuation of laser energy.

1.3 Surface scanning of the blast furnace pig iron samples without detailed composition

One cylindrical pig iron sample was got from the taphole runner of blast furnace. As shown in Fig.2(a), the surface of solidified pig iron sample was rough, which was unbeneficial for the LIBS detection. Thus, Wire Electrical Discharge Machining (WEDM) was adopted to cut the iron sample at different height and sanding were adopted to get a plat surface. Finally, two round iron samples were placed on the 3D moving stage for LIBS surface scanning analysis. The distance between the adjacent laser ablation points was 2 mm. At the edge of the sample, the ablation points became denser and the distance between them turned to be 1 mm or 0.5 mm. The surface morphology of iron samples after laser ablation were shown in Fig.2(b) and (c).

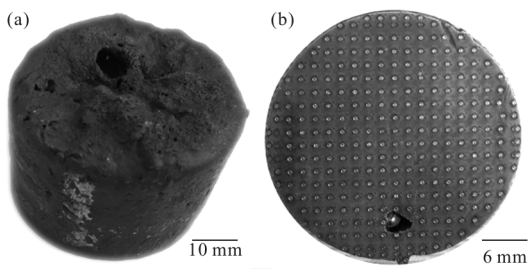

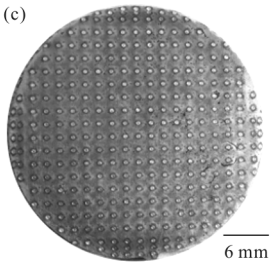

Fig.2 Original iron sample (a) and the morphology of round iron sample-1 (b) and sample-2 (c) after laser ablation

2 Results and discussion

2.1 LIBS spectra of pig iron

The typical LIBS spectra of pig iron was shown in Fig.3. The spectra was the cumulative results of 50 pulses. As can be seen in Fig.3, the LIBS spectra lines were very rich because of the existence of large amounts of matrix Fe lines. The existence of Fe lines may interfere with the spectra lines of other alloy elements if the wavelength of them are close to each other. Thus, the lines which were close to Fe spectra lines can't be selected as analytical lines for calibration.

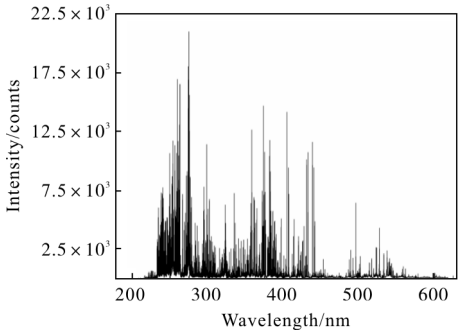

Fig.3 Typical LIBS spectra of pig iron

2.2 Calibration results of Si, Mn and Ti concentrations

The most widely used calibration method is internal standardization which could decrease the influence of matrix effect and the fluctuation of experimental condition effectively. The charac - teristic lines of matrix Fe are always chosen as the reference lines. Mathematical models are estab - lished based on the intensity radio ($I_{Si,\ Mn,Ti}/I_{Fe}$) and

the corresponding element concentration ($C_{Si,Mn,Ti}$) by least square regression method. The calibration model can be linear, quadratic cubic or logarithmic etc., which is decided by the self-absorption effect. The spectra including some common characteristic lines of alloy elements and matrix Fe were shown in Fig.4 in detail. According to the selection principle in other relative studies [17-18], the analytical lines and reference lines shown in Tab.2 were selected finally. Fe I 263.58 nm, Fe I 441.51 nm and Fe I 370.79 nm are the reference lines of Si I 288.16 nm, Mn I 293.31 nm and Ti II 334.94 nm, respectively.

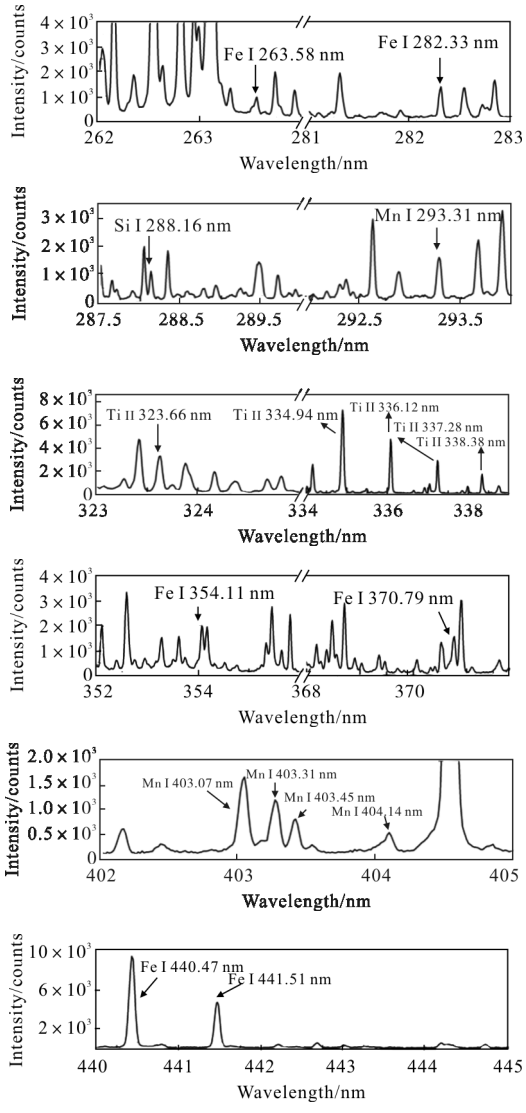

Fig.4 Common characteristic lines of Si, Mn, Ti and Fe in LIBS spectra

Tab.2 Spectral parameters of analytical and reference lines selected for calibration

Spectral line /nm	E_i/eV	E_j/eV	A_{ji}/s^{-1}	g_j
Fe I 263.58	0.990	5.693	2.11E+7	7
Fe I 441.51	1.608	4.416	1.19E+7	7
Fe I 370.79	2.176	5.519	3.32E+7	5
Si I 288.16	0.781	5.083	2.17E+8	3
Mn I 293.31	1.175	5.401	2.04E+8	3
Ti II 334.94	0.049	3.750	1.68E+8	12

The quadratic regression was conducted between intensity ratio and element concentration. The regression equations and coefficients of determination (R^2 factors) were shown in Fig.5. As shown in Fig.5, the R^2 factors of the calibration

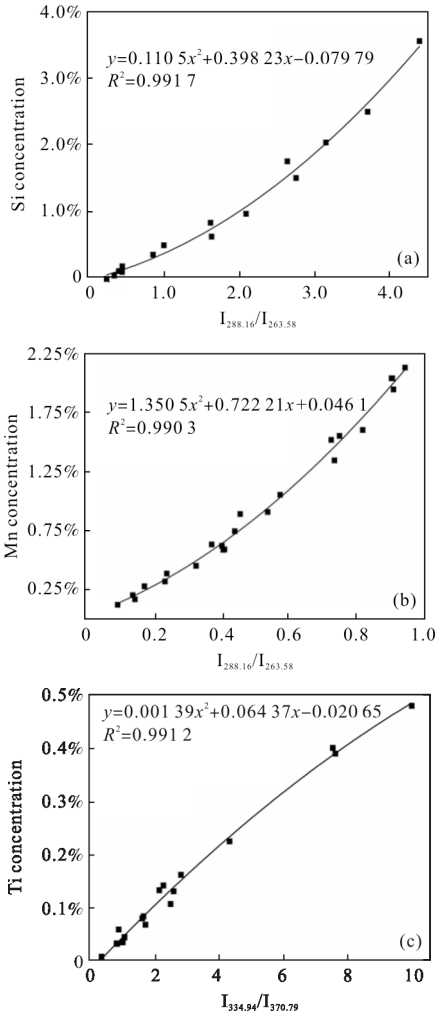

Fig.5 Calibration curves for the detection of Si, Mn and Ti in iron

curves were all larger than 0.99, which proved the ability of LIBS on simultaneous detection of Si, Mn and Ti concentrations.

2.3 Si, Mn and Ti segregation mapping by LIBS surface scanning analysis

LIBS system with 3D moving sample stage can realize the surface analysis of element concentration, based on which quantitative information about element segregation could be gotten. In this work, LIBS ablation was conducted in almost 300 different positions for each iron sample. The Si, Mn and Ti concentrations in these ablation points were calculated based on the regression equations in Fig.5 above. The results were displayed in form of images where the color scale was related directly to the element concentrations. The data between the ablation points were calculated by interpolation.

As shown in Fig.6 and Fig.7, the distribution of Si, Mn and Ti in solidified pig iron was heterogeneous. The positive segregation means the concentration in the detecting position is higher than the average concentration while the negative

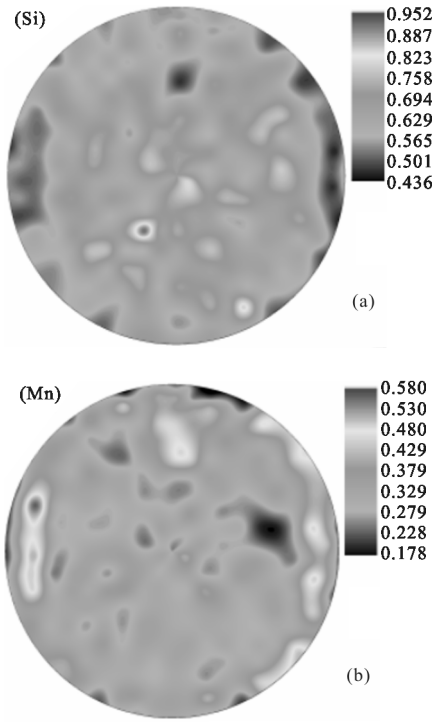

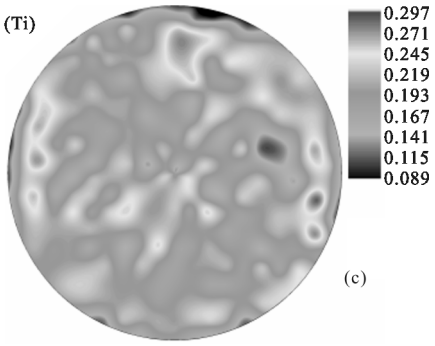

Fig.6 Si, Mn and Ti concentration maps of sample-1

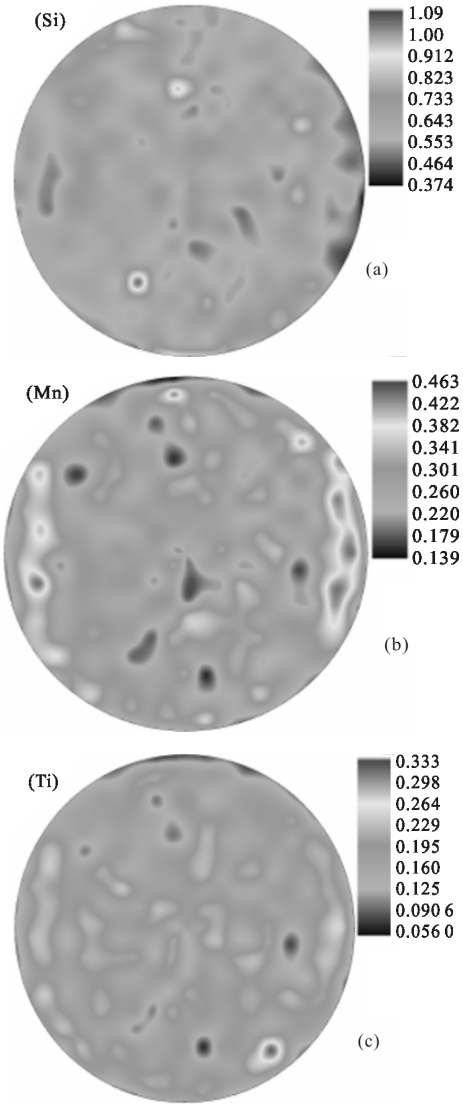

Fig.7 Si, Mn and Ti concentration maps of sample-2

segregation means the concentration in the detecting position is lower. Thus, the light color parts in these figures represented the positive segregation regions. The dark color parts

represented the negative segregation parts. It seems that no significant macro segregation phenomenon like central segregation was found in the element maps. The segregation appeared just in some local regions of the iron samples. During the sampling process of liquid iron, the solidification speed of iron was very fast and the final products was white iron, in which macro segregation is not serious. The results in this work may be caused by the micro segregation between grains. In addition, as can be seen in Fig.6 and 7, the negative segregation region of Si was just the positive segregation location of Mn, Ti, and it was also applicable in reverse.

Segregation degree is an important parameter used to evaluate the element segregation degree. It was calculated based on the following equation.

$$K_i = \frac{C}{C_0}$$

where K_i was the segregation degree of one kind of element in a certain location, C was the element concentration in a certain location, C_0 was the average element concentration of the sample. If parameter K_i equaled to 1, that meant there was no significant segregation in the pig iron sample. Thus, comparison between the value of K_i with 1 could reflect the positive and negative segregation degree. Based on the equation above, the maximum segregation degree was calculated and results were shown in Tab.3, where '+' represented maximum positive segregation, while '-' represented maximum negative segregation.

Tab.3 Maximum positive and negative degree of three elements in two round iron samples

Sample	Si		Mn		Ti	
	+	−	+	−	+	−
1	1.518	0.696	1.779	0.549	1.514	0.456
2	1.735	0.595	1.654	0.499	1.890	0.323

As can be seen in Tab.3, the segregation degree in some local region was serious. It revealed that we should measure at as more positions as possible and average the results when detect the element concentration of the whole sample. It was because the ablation area of laser was usually hundreds of micrometers, which may be easily affected by segregation regions. However, there was little difference between the maximum segregation degree in sample 1 and 2, and the segregation locations of sample 1 and 2 were similar with each other for three alloy elements. It meant there was little difference between the element maps at different height of the iron sample.

3 Conclusions

In this paper, quantitative analysis of Si, Mn and Ti segregation in pig iron was carried out with the help of spatial-resolved LIBS setup. The widely used internal standardization method was applied in calibration process of this work to reduce the influence of matrix effect and fluctuation of experiment condition. Based on the detailed spectra, parameters of common lines and experience of other researchers, Si I 288.16 nm, Mn I 293.31 nm and Ti II 334.94 nm were finally selected as the analytical spectra lines of three alloy elements, and Fe I 263.58 nm, Fe I 441.51 nm, Fe I 370.79 nm were adopted as their reference lines. The calibration curves for Si, Mn and Ti in standard pig iron samples exhibited a good quadratic fit, and the R^2 factors are 0.991 7, 0.990 3, 0.991 2, respectively.

The positive and negative segregation regions of round pig iron samples were shown clearly in the element maps by LIBS, and the maximum segregation degree was also calculated. The maximum segregation degree of sample-1 and 2 showed little difference with each other. In

addition, it seems that Si segregation law was opposite with Mn and Ti in pig iron. The negative segregation region of Si were just the positive segregation region of Mn and Ti, especially in the edge of the iron samples.

References:

[1] Choudhary S K, Ganguly S. Morphology and segregation in continuously cast high carbon steel billets [J]. ISIJ International, 2007, 47(12): 1759-1766.

[2] Kajatani T, Drezet J M, Rappaz M. Numerical simulation of deformation-induced segregation in continuous casting of steel [J]. Metallurgical and Materials Transactions A, 2001, 32(6): 1479-1491.

[3] Ludlow V, Normanton A, Anderson A, et al. Strategy to minimise central segregation in high carbon steel grades during billet casting [J]. Ironmaking & Steelmaking, 2005, 32(1): 68-74.

[4] Hou Guanyu, Wang Ping, Tong Cunzhu. Progress in laser-induced breakdown spectroscopy and its applications [J]. Chinese Optics, 2013, 6(4): 490-500. (in Chinese)

[5] Li Zhanfeng, Wang Ruiwen, Deng Hu, et al. Laser induced breakdown spectroscopy of Pb in Coptis chinensis [J]. Infrared and Laser Engineering, 2016, 45 (10): 1006003. (in Chinese)

[6] Yuan Di, Gao Xun, Yao Shuang, et al. The detection of heacy metals in soil with laser induced breakdown spectroscopy [J]. Spectroscopy and Spectral Analysis, 2016, 36(8): 2617-2620. (in Chinese)

[7] Dell'Aglio M, Gaudiuso R, Senesi G S, et al. Monitoring of Cr, Cu, Pb, V and Zn in polluted soils by laser induced breakdown spectroscopy (LIBS) [J]. Journal of Environmental Monitoring, 2011, 13(5): 1422-1426.

[8] Li Wenhong, Shang Liping, Wu Zhixiang, et al. Determination of Al and Fe in cement by laser-induced breakdown spectroscopy [J]. Infrared and Laser Engineering, 2015, 44(2): 508-512. (in Chinese)

[9] Mohamed W T Y. Improved LIBS limit of detection of Be, Mg, Si, Mn, Fe and Cu in aluminum alloy samples using a portable Echelle spectrometer with ICCD camera[J]. Optics & Laser Technology, 2008, 40(1): 30-38.

[10] Liu Li, Xiao Pingping. Accuracy improvement of temperature calculation of the laser-induced plasma using wavelet transform baseline subtraction [J]. Spectroscopy and Spectral Analysis, 2016, 36(2): 545-549. (in Chinese)

[11] Hao Z Q, Li C M, Shen M, et al. Acidity measurement of iron ore powders using laser-induced breakdown spectroscopy with partial least squares regression [J]. Optics Express, 2015, 23(6): 7795-7801.

[12] Rai N K, Rai A K. LIBS—an efficient approach for the determination of Cr in industrial wastewater [J]. Journal of Hazardous Materials, 2008, 150(3): 835-838.

[13] Li X, Yin H, Wang Z, et al. Quantitative carbon analysis in coal by combining data processing and spatial confinement in laser-induced breakdown spectroscopy [J]. Spectrochimica Acta Part B: Atomic Spectroscopy, 2015, 111: 102-107.

[14] Chen Shihe, Lu Jidong, Zhang Bo, et al. Controllable factors in detection of pulverized coal flow with LIBS [J]. Optics and Precision Engineering, 2013, 21 (7): 1651-1658. (in Chinese)

[15] Emde Benjamin, Hermsdorf Jörg, Kaierle Stefan. Identification of the zinc dispersion in rubber blends by libs with a Nd:YAG laser[J]. Chinese Optics, 2015, 8(4): 596-602.

[16] Boué-Bigne F. Laser-induced breakdown spectroscopy applications in the steel industry: Rapid analysis of segregation and decarburization [J]. Spectrochimica Acta Part B: Atomic Spectroscopy, 2008, 63(10): 1122-1129.

[17] Boué-Bigne F. Simultaneous characterization of elemental segregation and cementite networks in high carbon steel products by spatially-resolved laser-induced breakdown spectroscopy [J]. Spectrochimica Acta Part B: Atomic Spectroscopy, 2014, 96: 21-32.

[18] Zhang Yong, Jia Yunhai, Chen Jiwen, et al. Segregation bands analysis of steel sample using laser-induced breakdown spectroscopy [J]. Spectroscopy and Spectral Analysis, 2013, 33(12): 3383-3387. (in Chinese)